# $^{13}C$- and Proton-ENDOR Studies of $^{13}C$-labelled Organic Radicals

H.-J. Fey, W. Lubitz *, H. Zimmermann **, M. Plato, K. Möbius, and R. Biehl
Institut für Molekülphysik, Freie Universität Berlin

Z. Naturforsch. **33a**, 514—522 (1978); received March 1, 1978

As part of a systematic non-proton ENDOR-in-solution study results are reported for $^{13}C$ in several isotopically enriched model compounds. Methods for synthesizing these labelled compounds are also presented. The optimum $^{13}C$ ENDOR temperatures are found to be considerably higher than for protons on account of the larger hyperfine anisotropy. Cross relaxation effects are used to determine rotational correlation times. The isotropic $^{13}C$ hyperfine couplings are in satisfactory agreement with INDO results.

## 1. Introduction

For the determination of electronic and geometrical structures of paramagnetic molecules the hyperfine interaction between unpaired electrons and nuclear magnetic moments in the molecule serve as a very powerful tool. For molecular systems with low symmetry detailed hyperfine information often cannot be obtained by standard ESR spectroscopy since too many unresolved lines lead to strongly inhomogeneously broadened spectra. In this case electron-nuclear-double-resonance (ENDOR) has proven to be of considerable help due to its much larger resolving power. Particularly in liquid solution the high resolution capability of the ENDOR method has made it possible to unravel the isotropic hyperfine structure of low symmetry organic radicals [1]. For experimental reasons ENDOR-in-solution was primarily confined to proton hyperfine interactions, and only more recently a variety of non-proton ENDOR experiments were successful [2—12]. $^{13}C$ is a particularly important nucleus in this respect, since it probes the value of the molecular wavefunction also at "blind" positions, i.e. at molecular positions which do not carry hydrogen atoms. Furthermore, $^{13}C$ hyperfine couplings are more sensitive to structural changes and dynamic effects arising from hindered rotation and/or ion pairing [13].

Experimental conditions for optimum ENDOR signal intensities depend strongly on the relaxation characteristics of the various nuclei. Such relaxation studies can provide additional structural information. As part of a systematic non-proton ENDOR study this paper reports results of $^{13}C$ nuclei in isotopically enriched model compounds. In the first part the methods for synthesizing these labelled compounds are described. In the second part the stationary $^{13}C$ hyperfine couplings and their interpretation in the INDO molecular orbital frame is presented, and in the third part the relaxation behaviour of $^{13}C$ ENDOR signals and its exploitation for the determination of rotational correlation times are reported.

## 2. Experimental

ENDOR and TRIPLE-resonance measurements were performed on home-built spectrometers described earlier [14, 15].

The radical anions **1** to **4** were generated by alkali metal reduction using standard techniques on a high vacuum line [16]. Dimethoxyethane (DME) was used as solvent. The triphenylmethyl radical **5** was prepared from the respective chloride by reaction with powdered silver, and the galvinoxyl radicals **6** and **7** were produced by oxidation using activated $PbO_2$. For the neutral radicals **5** and **7** toluene was used as solvent. To prevent boiling, the sample tubes were filled with purified nitrogen of 760 Torr. The structure of radicals investigated is shown in Figure 1.

The synthesis of compounds from which radicals **1** to **5** were generated is presented in the following section, the synthesis of **6** and **7** has been described earlier [11].

### *1. $^{13}C$-carboxyl-perdeuterobenzophenone* [17]

$^{13}C$ enriched perdeuterobenzoic acid was prepared from perdeuterobromobenzene, $D = 99\%$, by Grignard reaction with $^{13}CO_2$, generated from $Ba^{13}CO_3$, $^{13}C = 90\%$. After chlorination by thionyl-

---

* Institut für Organische Chemie, Freie Universität Berlin.

** Max-Planck-Institut für Medizinische Forschung, Heidelberg.

Requests for reprints should be addressed to Prof. K. Möbius, Institut für Molekülphysik, Freie Universität Berlin, Boltzmannstr. 20, D-1000 Berlin 33, Germany.

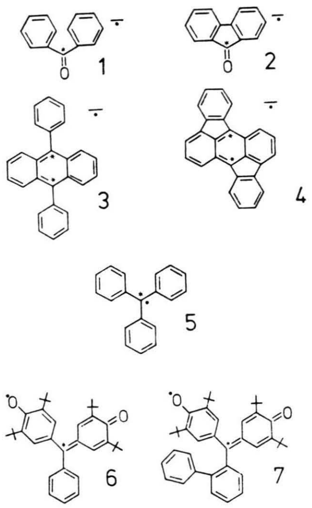

Fig. 1. Structure of radicals investigated.
**1**: $^{13}$C-carbonyl-perdeuterobenzophenoneketyl,
**2**: 9-$^{13}$C-perdeuterofluorenoneketyl,
**3**: 9,10-di-$^{13}$C-perdeutero-9,10-diphenyl-anthracene radical anion,
**4**: 7b,14b-di-$^{13}$C-perdeuterorubicene radical anion,
**5**: α-$^{13}$C-perdeuterotriphenylmethyl,
**6**: $^{13}$C-phenylgalvinoxyl,
**7**: $^{13}$C-2-biphenylylgalvinoxyl, galvinoxyl: (3,5-di-tert-butyl-4-oxocyclohexa-2,5-dienyliden)-(3,5-di-tert-butyl-4-oxyphenyl)-methyl.
* 13C-positions

chloride, the resulting benzoylchloride was alkylated by Friedel-Kraft's reaction with perdeuterobenzene and $AlCl_3$ to yield benzophenone-$d_{10}$-$^{13}$C-carbonyl. The product was purified by vacuum sublimation and subsequent zone refinement under nitrogen.

$$^{13}C = 90\%; \quad D = 99\%, \quad m/e^{\oplus} = 193.$$

### *2. 9-$^{13}$C-perdeuterofluorenone*

a) Diphenyl-2-$^{13}$C-carboxylic acid

A Grignard solution was prepared from 2.6 g magnesium chips and 30.6 g 2-jodobiphenyl in 180 ml dry diethylether. It was diluted with 200 ml methylenechloride, and this solution was then carboxylated under stirring and cooling at −60 °C with $^{13}CO_2$ generated by reaction of $H_2SO_4$ on $Ba^{13}CO_3$ (25 g "$^{13}$C 90%"). The reaction was carried out in a high vacuum manifold system. To make sure, there was a complete carboxylation, the temperature was kept at −60 °C for 4 hours, then approximately 2 hours before the hydrolysis at −10 °C to −20 °C. The reaction product was worked up in the usual manner and yielded 14.5 g diphenyl-2-$^{13}$C-carboxylic acid.

b) Oxidation to 9-$^{13}$C-fluorenone

Diphenyl-2-$^{13}$C-carboxylic acid (11 g) and 40 ml sulphuric acid conc. were stirred at 80 °C for 20 minutes and poured in 800 ml ice-water under continuing stirring. The separated fluorenone was dissolved in diethylether, three times extracted with 1 n NaOH and subsequently with water. The dried extract was evaporated to yield 8.5 g 9-$^{13}$C-fluorenone.

$$m/e^{\oplus} = 181, \quad Fp = 82-83\ ^{\circ}C.$$

c) Reduction to 9-$^{13}$C-fluorene

9-$^{13}$C-fluorenone in 200 ml ethyleneglycole was refluxed together with 30 ml dry hydrazin-hydrat for 8 hours. The fluorene sublimed in the cooler, was dissolved with diethylether, extracted with 2*n* HCl, subsequently with water and the solvent was evaporated.

Yield = 7 g,
Fp = 114−115 °C (after two sublimations),
$m/e^{\oplus} = 167$.

d) 9-$^{13}$C-perdeutero fluorene

Fully deuterated fluorene was prepared by hydrogendeuterium exchange with large excess of $D_2O$ and $PtO_2$ as catalyst, which was prereduced with deuterium gas. The mixture was heated in a high pressure system at 350 °C. The repeated reaction yielded highly deuterated fluorene in good chemical and isotopic yield.

e) 9-$^{13}$C-perdeuterofluorenone

1.0 g 9-$^{13}$-C-perdeuterofluorenone dissolved in 2 ml boiling acetic acid-$d_1$ was oxidized slowly drop by drop with sodium dichromate (3 g) in $CH_3COOD$ 80% in $D_2O$ (5 ml). The mixture was refluxed for 2 hours and the dark green solution was poured into ice-water (100 ml). The precipitated fluorenone was recrystallized twice from methanol.

$$Fp = 80-81\ ^{\circ}C, \qquad Yield = 750\ mg,$$
$$m/e^{\oplus} = 189, \qquad ^{13}C = 90\%, \qquad D = 98-99\%.$$

### *3. 9.10-Di-$^{13}$C-perdeutero-9.10-diphenylanthracene*

According to a procedure of W. Schlenk [18]: 120 mg calcium splinters and 360 mg $^{13}$C-perdeuterobenzophenone were refluxed at about 300 °C

---

* The postitions with an asterisk are $^{13}$C-labelled.

for one hour. The cooled mixture was extracted twice with hot benzene and after evaporation of the solvent, the residue was purified by chromatography on neutral alumina and benzene as the eluent, yellow crystals.

Yield = 40 mg, Fp = 239–240 °C,
$m/e^{\oplus}$ = 350/100% 349/25% 348/11%.

The 9.10-$^{13}$C-diphenylanthracene contains approximately 80% two $^{13}$C and about 10% one $^{13}$C.

### 4. *7b.14b-Di-$^{13}$C-perdeuterorubicene* [19]

0.6 g 9-$^{13}$-C-perdeutero fluorenone was thoroughly mixed with 300 mg highly pulverized calciumhydride in a test tube. The lower part of the test tube was heated by an open flame. The melt was refluxed for several minutes and the deep red rubicene sublimed to the upper part of the tube. The stiffened melt was then pulverized and extracted with 20 ml cold methylalcohol. The residue was extracted twice with boiling xylene and out of the filtrated red solution the $^{13}C_2$-rubicene crystallized in bright needles.

Yield = 100 mg, Fp = 305–306 °C,
$m/e^{\oplus}$ = 342/62% 341/100% 340/92% 339/62%.

The rubicen contains to 80% two $^{13}$C in the positions 7b and 14b and to 10% one $^{13}$C. There was a little exchange during the reflux with $CaH_2$. The contents of deuterium is 95%.

The 7b, 14b-$^{13}C_2$-rubicene-prot. was synthesized in the same way starting from 9-$^{13}$C-fluorenone.

$m/e^{\oplus}$ = 328, Fp = 305–306 °C.

a) $^{13}$C-perdeuterobenzhydrole [20]

3.2 g $^{13}$C-benzophenoneperdeutero was reduced in 50 ml anhydrous tetrahydrofurane to the corresponding deuterated alcohol by $LiAlD_4$ at 0 °C. $D_2O$ 99.5% was used to decompose the excess $LiAlD_4$ and worked up in the usual manner. Recrystallization from petrolether yielding 3 g. $^1$H-NMR shows complete deuteration including OD.

Fp = 66 °C–67 °C.

b) α-$^{13}$C-perdeuterotriphenylmethane [21]

A solution of 3 g $^{13}$C-perdeuterobenzhydrole and 50 ml hexadeuterobenzene was stirred and cooled at +4 °C. 2.2 g anhydrous $AlCl_3$ was added in small portions during a period of 2 hours. The mixture was stirred at +4 °C for 90 minutes, was worked up with 50 g ice and after three extractions with benzene ($h_6$, 3 times) the solvent was evaporated. Purification and the separation from traces of anthracene which is formed simultaneously was done by chromatography with silica gel; eluent: cyclohexane.

Yield = α-$^{13}$C-perdeuterotriphenylmethane 2.8 g.
Fp = 93–94 °C, $m/e^{+}$ = 261, $^{13}$C 90%,
D 99%.

c) α-$^{13}$C-perdeuterotriphenylmethylchloride [3]

840 mg $^{13}$C-perdeuterotriphenylmethane was refluxed with 4 ml sulphurylchloride and 25 mg benzoylperoxide for 90 minutes. The excess sulphurylchloride was separated by distillation under reduced pressure. The residue was recrystallized twice from benzene/petrolether (b.p.) 40 °C.

Yield = 150 mg, Fp = 101–108 °C,
$m/e^{\oplus}$ = 261; 259.

## 3. Results and Discussion

### 1. *Interpretation of Isotropic Hyperfine Coupling Constants*

The ENDOR results for the $^{13}$C-hyperfine couplings (hfcs) of the various compounds are collected in Table 1. Theoretical values obtained by the INDO-MO-method [22] are also given for one typical representative of each group of radicals (neutral, hydrocarbon ion, and ketyls).

a) Neutral Radicals

Triphenylmethyl **5**: Using standard bond angles and lengths and a twist angle for the phenyl rings of 40° obtained from neutron and X-ray scattering [23, 24] the INDO calculation reproduces our experimental $^{13}$C-hfc quite well. Good agreement between theoretical and experimental proton-hfcs was only obtained for the para position. For the other two H-hfcs in the ortho and meta position INDO fails, probably due to the over estimation of $\pi$-$\sigma$-mixing [25]. The sign of the temperature coefficient of the $^{13}$C-hfc is also consistent with the calculation, since increasing the twist angle yields a larger $^{13}$C-hfc. It is evident that the mean twist angle will increase towards higher temperatures [26]. — Our measured $^{13}$C-hfc is in agreement with recent experimental results found in other solvents [26].

Table 1. Experimental and theoretical $^{13}$C-hyperfine couplings.

| Radical[a] (solvent) | Experiment[b] | | Theory (INDO)[d] |
|---|---|---|---|
| | $a_C$/MHz | $da_C/dT$ kHz · K$^{-1}$[c] | $a_C$/MHz |
| 1 (Li$^+$/DME) | $+32.51 \pm 0.03$ | $+23.7 \pm 0.1$ | |
| 2 (Li$^+$/DME) | $+17.66 \pm 0.03$ | $+21.4 \pm 0.1$ | $+19.12$ |
| 3 (K$^+$/DME) | $+25.84 \pm 0.03$ | | |
| 4 (K$^+$/DME) | $+16.42 \pm 0.03$<br>$(+19.90)$[e] | $+\ 3.6 \pm 0.1$ | $+22.76$ |
| 5 (toluene) | $+66.87 \pm 0.1$ | $+17.0 \pm 0.3$ | $+65.55$ |
| 6 (toluene) | $-27.77 \pm 0.03$ | $-\ 1.3 \pm 0.1$ | |
| 7 (toluene) | $-27.38 \pm 0.03$ | $-\ 2.6 \pm 0.1$ | |

[a] See Fig. 1 for names and structural formulas.
[b] Temperature 300 K, the signs of the $^{13}$C-hfcs were determined from linewidth variations in the ESR spectra.
[c] The temperature was varied between 220 and 360 K.
[d] For INDO calculations see text.
[e] Value from the non-deuterated radical.

### b) Ketyls

Fluorenone ketyl 2: As has been shown earlier, fluorenone ketyl forms contact ion pairs in ethereal solutions even at temperatures as high as 300 K and irrespective of the type of counter ion [27]. All hfcs — especially the $^{13}$C-hfc in the keto group — are strongly influenced by the type and position of the counter ion. We have therefore performed INDO calculations with the lithium counter ion placed in different positions near the keto group which is the region of strongest electrostatic attraction. Bond lengths and angles of the ketyl were taken form crystallographic data [28]. The mean square deviation of the calculated hfcs from the experimental values — including also the $^{17}$O- and $^7$Li-hfcs — showed a minimum when placing the lithium-cation at the position $x = 1.0$ Å, $y = 0.0$ Å, $z = 2.0$ Å; the corresponding $^{13}$C-hfc is given in Table 1. The coordinate system was centered on the oxygen atom with the $x$-axis along the O—C bond and the $xy$-plane in the molecular plane. The dynamics of the ion pair and the influence of solvent were not accounted for in the calculation. Nevertheless, we believe the calculated position to be realistic and that the INDO method can be used for the elucidation of ion pair structures in such radicals. More detailed investigations on such systems will be published in due course [29]. Up to now INDO calculations can only be performed on "first row" elements. Therefore no calculations of this type could be performed on sodium and heavier counter ions.

### c) Hydrocarbons

Rubicene radical anions: In Table 2 the experimental H- and $^{13}$C-hfcs for the non-deuterated rubicene radical anion (K$^+$/DME) are compared with those calculated by the INDO method. For this calculation we used standard bond lengths and angles, except for the five membered rings, where 1.46 Å was chosen for the connections to the benzene rings [30]. The agreement between measured and calculated hfcs is quite satisfactory except for positions 2, 4 and 6, where the theoretical values come out too large in the positive sense. In the case of position 2 this even results in a sign reversal. It is our experience [8, 13] that the INDO method tends to exaggerate positive contributions to the proton 1s spin populations at positions with small hyperfine couplings ($a < 2$ MHz). Furthermore, it is known that condensed aromatic systems containing five-membered rings which link six-membered benzenoid structures usually contain abnormally long C—C-bonds [28, 30]. The weakened $\pi$-bonding in these rings may imply that a non-planar configuration prevails. Such configurations were not considered in our calculations but might also explain the partial disagreement between theory and experiment. Nevertheless, we believe our assignment of the hfcs to be acceptable since they agree well in sign and relative magnitude with those measured in the anthracene anion [31] and

Table 2. Experimental and theoretical H- and $^{13}$C-hfcs of the rubicene anion radical.

| Position | $a$/MHz | |
|---|---|---|
| | Experiment | Theory (INDO) |
| $H_{1,8}$ | $-\ 6.61$ | $-\ 8.41$ |
| $H_{2,9}$ | $-\ 2.27$ | $+\ 0.70$ |
| $H_{3,10}$ | $-\ 5.75$ | $-\ 5.38$ |
| $H_{4,11}$ | $+\ 0.45$ | $+\ 1.77$ |
| $H_{5,12}$ | $-\ 3.31$ | $-\ 3.42$ |
| $H_{6,13}$ | $+\ 0.22$ | $+\ 0.98$ |
| $H_{7,14}$ | $-\ 3.03$ | $-\ 3.03$ |
| $C_{7b,14b}$ | $+19.90$ | $+22.76$ |

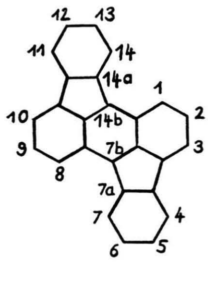

the fluorenone ketyl [32], radicals from which the rubicene anion structure is composed. It should be mentioned that the $^{13}$C-hfc measured in the perdeuterated rubicen anion **4** was only $+16.42$ MHz as compared with 19.90 MHz in the non-deuterated compound (see Table 1). This very large isotopic effect needs further clarification and will not be discussed here.

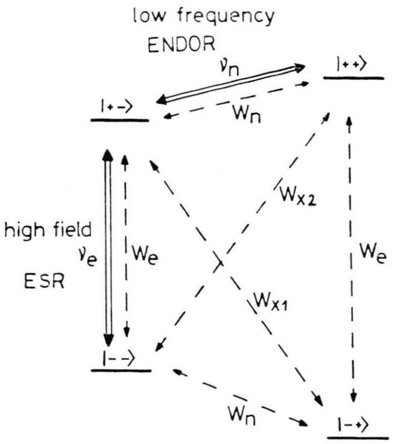

Fig. 2. Energy level system for $S=\frac{1}{2}$, $I=\frac{1}{2}$ in a high nagnetic field, showing induced ESR ($\nu_e$) — and NMR ($\nu_n$) — transitions and all possible spin lattice relaxation paths; isotropic hyperfine coupling $a>0$, $|a/2|>|\nu_{\text{free nucleus}}|$.

### 2. *Relaxation Effects*

#### a) Spin Lattice Relaxation Rates

The amplitude of an ENDOR signal depends strongly on the various spin-lattice relaxation rates $W_{ij}$ coupling the different pairs of energy levels $i$, $j$ of the spin system. The most important mechanism in liquid solutions for producing such relaxation rates is Brownian rotational diffusion. This mechanism modulates the anisotropic Zeeman and hyperfine interactions and the ensueing relaxation rates therefore depend on the traceless parts of the $g$-tensor and dipolar hyperfine tensors, $\mathbf{G}$ and $\mathbf{A}$ (for nuclei with $I<1$ such as protons and $^{13}$C, there is no quadrupolar contribution).

We consider the simplest possible spin system containing just one electron spin $S=1/2$ and nuclear spin $I=1/2$. This is a sufficiently good model for the radicals **1**, **2**, **5**, **6**, and **7** which contain only one $^{13}$C nucleus and where the deuterium nuclei or protons can be neglected on account of their comparatively small hyperfine couplings (Trace $\mathbf{A}^2(\mathrm{D}) \lesssim 10^{-1}$ Trace $\mathbf{A}^2(\mathrm{H}) \lesssim 10^{-2}$ Trace $\mathbf{A}^2(^{13}\mathrm{C})$, see below). For this four-level system, relaxation theory [32] gives generally the following five different relaxation rates (see Fig. 2)

$$W_n = \frac{1}{40}\operatorname{Tr}\mathbf{A}^2\,\tau_c\,, \tag{1a}$$

$$W_{e_{1/2}} = \left[\frac{1}{10}(\beta_e B_0/\hbar)^2 \operatorname{Tr}\mathbf{G}^2 \pm \frac{1}{10}\beta_e B_0/\hbar \operatorname{Tr}(\mathbf{GA}) + \frac{1}{40}\operatorname{Tr}\mathbf{A}^2\right]\frac{\tau_c}{(1+\omega_e^2\tau_c^2)}\,, \tag{1b}$$

$$W_{x_2} = \frac{1}{10}\operatorname{Tr}\mathbf{A}^2\,\frac{\tau_c}{1+\omega_e^2\tau_c^2}\,, \tag{1c}$$

$$W_{x_1} = \frac{1}{6}W_{x_2}\,, \tag{1d}$$

where $\mathbf{A}$ is given in rad · sec$^{-1}$, $\operatorname{Tr}\mathbf{AB} = \sum_{r,s} A_{rs}B_{rs}$, $\tau_c$ is the rotational correlation time in sec and $\omega_e$ is the electron transition frequency in rad · sec$^{-1}$. There is an additional important contribution to $W_e$ from spin-rotational interaction given by [32]

$$W_e^{\mathrm{SR}} = \frac{1}{18}\sum_i (g_{ii}-g_e)^2\,\tau_c^{-1}\,, \tag{2}$$

where $g_{ii}$, $i=1, 2, 3$, are the principal values of the $g$-tensor and $g_e$ is the free electron $g$-factor. Finally, there may be a modulation of the isotropic coupling constant $a$ of the $^{13}$C nucleus by intramolecular reorientation processes. This would produce an additional contribution to $W_{x_1}$ given by [33]

$$W_{x_1}^{\mathrm{I}} = \frac{1}{2}\left(\overline{a^2(t)} - \overline{a(t)}^2\right)\frac{\tau_\mathrm{I}}{1+\omega_e^2\tau_\mathrm{I}^2}\,, \tag{3}$$

where $\tau_\mathrm{I}$ is the characteristic correlation time for this modulation process.

The rotational correlation time $\tau_c$ can be estimated from the Debye relation

$$\tau_c = \frac{4}{3}\pi r_0^3\,\eta/kT\,, \tag{4}$$

where $r_0$ is an effective spherical radius of the tumbling solvated molecule and $\eta$ is the viscosity of the solvent.

#### b) Optimization of ENDOR-signals

Maximum ENDOR signals are obtained for $W_n \simeq W_e$ when cross relaxation processes $W_{x_1}$

and/or $W_{x_2}$ are negligible. In the slow tumbling limit $\omega_e \tau_c \gg 1$ for ESR-transitions, which is normally realized in proton ENDOR studies, cross relaxation caused by rotational diffusion plays a minor role in comparison with $W_n$. From Eqs. (1a) and (2) it follows that $W_n/W_e \propto \mathrm{Tr}\,\mathbf{A}^2 \tau_c^2$, provided $W_e^{\mathrm{SR}} > W_{e_{1/2}}$. This condition is generally fulfilled for the systems studied here [34]. Since Tr $\mathbf{A}^2$ is usually much larger for $^{13}$C than for protons one therefore expects maximum ENDOR signals for $^{13}$C at more elevated temperatures than for protons. This is confirmed by our experiments. The ENDOR lines of all molecules **1** to **7** attained their maximum between 270 and 340 K whereas proton ENDOR is normally observed around 200 K in the same solvent, e.g. DME or toluene. Figure 3 shows the experimental ENDOR enhancement (ENDOR signal amplitude/ESR signal amplitude) as a function of $\eta/T$.

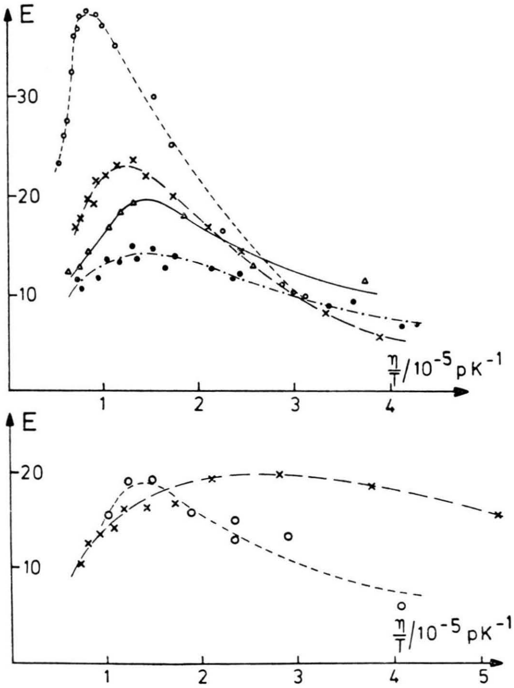

Fig. 3. ENDOR enhancement $E$ in arbitrary units vs. $\eta/T$ of the solution. Top: ○: **1**, Li$^+$ counterion; ×: **1**, K$^+$; △: **2**, Li$^+$; ●: **4**, K$^+$. Bottom: ○: **5**; ×: **6**.

For structurally similar molecules like the ketyls one expects a near proportionality between the isotropic $^{13}$C coupling $a_c$ and the principal value of the dipolar hyperfine tensor $\mathbf{A}$, since for the studied molecules both are mainly determined by the $\pi$-spin density on the $^{13}$C atom itself. The optimum value of $\tau_c^{-1}$ and thus of $T/\eta$ should therefore be nearly proportional to $a_c$. This is well confirmed experimentally (Figure 4).

### c) Cross Relaxation Effects in $^{13}$C-ENDOR

As can be seen from Fig. 5, the relative amplitudes of the $^{13}$C-ENDOR lines depend markedly on which of the two components of the ESR-$^{13}$C-doublet is irradiated. The high-(low-) frequency ENDOR line is always more intense than the other when irradiating the low-(high-) field ESR line.

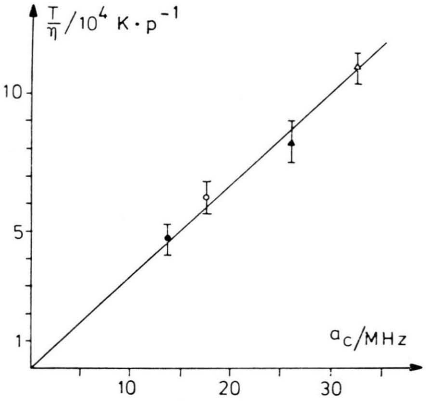

Fig. 4. Correlation between $T/\eta$ for maximum ENDOR enhancement and the isotropic $^{13}$C-hfc of radicals **1**, Li$^+$ counterion (○); **1**, K$^+$ (●); **2**, Li$^+$ (△); **2**, K$^+$ (▲). From the slope one obtains

$$a_c \cdot \eta/T = 2.97 \times 10^{-4}\ \mathrm{MHz} \cdot \mathrm{p} \cdot \mathrm{K}^{-1} \pm 5\%.$$

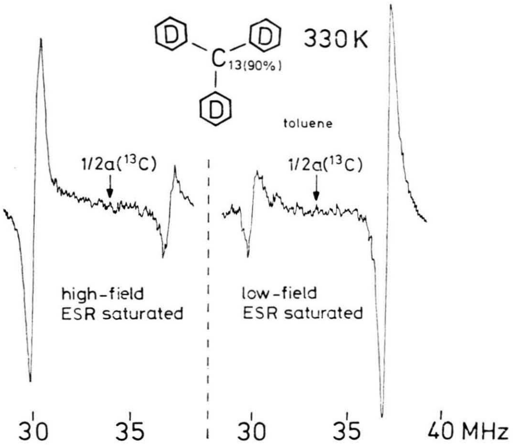

Fig. 5. $^{13}$C-ENDOR spectra of the triphenylmethylradical **5** when saturating the two different ESR $^{13}$C-hyperfine components. The two $^{13}$C-ENDOR lines are separated by twice the free nuclear resonance frequency of $^{13}$C and centered around $a$ ($^{13}$C)/2.

This effect, which has also been observed on other systems [2, 3, 4, 8], shows the existence of a dominating $W_{x_2}$ cross relaxation process. It follows from Eqs. (1d) and (3) that this is only possible if the molecular tumbling motion is the dominant source for cross relaxation.

Measurements of the ratio $R(\geqq 1)$ of the high- and low-frequency ENDOR lines as a function of $\eta/T$ can yield $\tau_c$ and $r_0$ of Eq. (4) provided $r_0$ can be taken as temperature independent. In comparison to other methods employing the $\tau_c$ dependence of absolute ESR linewidths [34] this method has the advantage of requiring only relative quantities. By applying the general method given by Freed for calculating the electron-nuclear saturation parameter $\Omega_{en}$ [35], the square of which directly determines the magnitude of the ENDOR signal, one obtains

$$R = S_2/S_1 \tag{5}$$

where

$$S_1 = [W_{x_1}(W_e + W_n + W_{x_2} + \omega_{HE}/4) + W_e W_n - W_{x_2}\,\omega_{HE}/4]^2$$

and $S_2$ is obtained from $S_1$ by interchanging subindices 1 and 2. It has been shown experimentally and theoretically [36] that within 10% $R$ is independent of the applied NMR-rf field. Eq. (5) takes into account effects of Heisenberg-exchange. The corresponding exchange rate $\omega_{HE}$ was inserted into the transition probability matrix $\boldsymbol{W}$ by the method described in [37]. We have furthermore asserted that terms in Eq. (1b) containing the tensor $\mathbf{G}$ give a negligible contribution to $W_e$ in view of the large $^{13}$C hyperfine anisotropy, which leaves us with a single

$$W_e = W_e^{SR} + \mathrm{Tr}\,\mathbf{A}^2\,\tau_c/[40(1 + \omega_e^2\,\tau_c^2)]\,.$$

If all relaxation and exchange rates in Eq. (5) are expressed in units of $W_n$ one is left with 3 parameters determining $R$:

$$\omega_e\,\tau_c\,,\quad \omega_e^2\,\tau_c^2\,W_e^{SR}/W_n \equiv b\,,$$
$$\omega_e^2\,\tau_c^2\,\omega_{HE}/W_n \equiv d\,,$$

where $b$ and $d$ should be independent of temperature (in highly dilute solution normally $\omega_{HE} \propto T/\eta \propto \tau_c^{-1}$ [34]). We now solve Eq. (5) for $\omega_e\tau_c$ which then becomes a function of the experimentally determined values of $R$ and the initially unknown parameters $b$ and $d$. If Eq. (4) is to hold, this function must be directly proportional to $\eta/T$. This restricts $b$ and $d$ to a *unique* set of values which were determined by trial and error. The final correlation between $\tau_c$ and $\eta$ is depicted in Fig. 6 for radical **2**, Li$^+$ counterion, as a typical example.

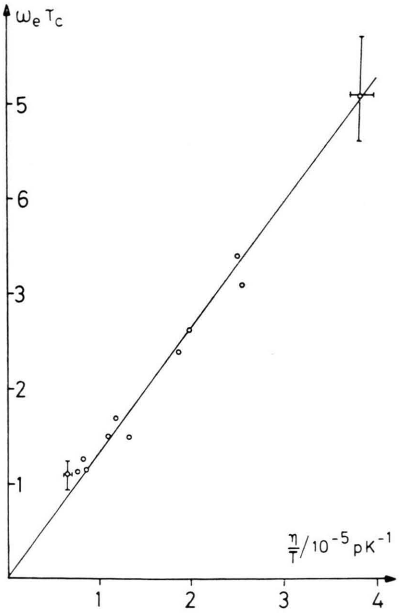

Fig. 6. Values of $\omega_e\tau_c$ — calculated from the intensity ratio $R$ [Eq. (5)] of the high frequency ENDOR line of **2**, Li$^+$ saturating the low/high-field ESR transition — as a function of $\eta/T$.

The value of $\tau_c/(\eta/kT) \equiv V_c$ taken from Fig. 6 and the corresponding values of $b$ and $d$ are listed in Table 3. Column 4 gives values for the molecular volumes $V_M$ calculated from the densities and molecular weights of the different compounds. It is

Table 3. Effective volumes of radicals calculated from relaxation effects ($V_c$) and from densities and molecular weights ($V_M$). For definition of $V_c$ and $V_M$ see text. Also listed are the fitting parameters $b$ und $d$ for the determination of $\tau_c$. For radicals **6** and **7** no reliable densities were available.

| Radical | $b$ | $d$ | $V_c$/Å$^3$ | $V_M$/Å$^3$ |
|---|---|---|---|---|
| **1** | 8 ± 1 | 2 ± 1 | 385 | 275 |
| **2** | 8 ± 1 | 2 ± 1 | 310 | 265 |
| **4** | 16 ± 4 | 2 ± 1 | 447 | 426 |
| **5** | 3.5 + 0.5 | 2 ± 1 | 315 | 256 |
| **6** | | | 618 | — |
| **7** | | | 660 | — |

interesting to compare these values with $\tau_c/(\eta/kT)$, which, according to Eq. (4), should be equal to an "effective" spherical volume $V_c = \frac{4}{3}\pi r_0^3$ of the tumbling solvated molecule. Both kinds of volumes agree quite well. However, $V_c$ appears to be systematically larger than $V_M$ by 10 to 20%, which could be attributed to an effective increase of the molecular volume by the solvation shell. The results for $b$ and $d$ are discussed elsewhere [36]. Here they will only be regarded as fitting parameters for the determination of $\tau_c$.

### d) Effects due to modulation of $a_{\mathrm{iso}}(^{13}\mathrm{C})$

The galvinoxyl radicals show an ENDOR amplitude ratio $R < 1$ at temperatures below 250 K. This can only be explained by assuming a modulation of the isotropic $^{13}$C-hfc giving rise to an additional $W_{x_1}$-process according to Equation (3). The corresponding correlation time $\tau_I$ at 250 K can be estimated from the activation energy $E_a = 1$ kcal/mol [38] for the hindered rotation of the phenoxyl groups in the unsubstituted galvinoxyl:

$$\tau_I = \tau_0\, e^{E_a/kT} = 6 \cdot 10^{-11}\ \mathrm{sec}$$

according to the classical jump model of Das [39] where the preexponential factor $\tau_0$ was taken to be about four times as large as that of benzophenone ($\tau_0 = 5 \cdot 10^{-11}$ sec) [40]. This gives $\omega_e \tau_I = 3$ whereas $\omega_e \tau_c \sim 15$ at the same temperature showing that in this case modulation of the isotropic coupling can become the dominant source of cross relaxation at such low temperatures on account of its higher spectral density at the electron transition frequency $\omega_e$.

## Conclusion

In conclusion one can state that under properly chosen experimental conditions $^{13}$C-ENDOR signals of radicals in solution can be obtained without serious difficulty. The optimum ENDOR temperatures are higher than for protons on account of the larger hyperfine anisotropy. At such temperatures pronounced cross-relaxation effects show up due to modulation of the anisotropic hyperfine interaction through molecular tumbling. On the basis of relaxation theory correlation times for molecular tumbling could be determined by measuring relative ENDOR amplitudes. From these correlation times and using the Debye formula, effective volumes of the solvated molecules could be estimated. In the case of the galvinoxyl radicals an additional modulation of the isotropic hfs coupling resulting from the hindered rotation of the phenoxyl groups could be observed. The $^{13}$C-ENDOR lines are generally broader and more difficult to saturate than proton lines. The experimental $^{13}$C-hfs data are in satisfactory agreement with INDO results.

### *Acknowledgement*

The authors are indebted to Prof. W. Broser (Inst. Org. Chem.) for the extension of the INDO program to larger molecules and his help in performing the calculations. Furthermore, we thank K. Schubert (Inst. Org. Chem.) for the preparation of the labelled galvinols. Financial support by the Deutsche Forschungsgemeinschaft (SFB 161) is gratefully acknowledged.

[1] L. Kevan and L. D. Kispert, Electron Spin Double Resonance Spectroscopy, John Wiley-Intersci., New York 1976.
[2] K. P. Dinse, K. Möbius, R. Biehl, and M. Plato, Proc. Congress Ampère **17**, 419 (1973).
[3] D. S. Leniart, J. C. Vedrine, and J. S. Hyde, Chem. Phys. Lett. **6**, 637 (1970).
[4] K. P. Dinse, K. Möbius, M. Plato, R. Biehl, and H. Haustein, Chem. Phys. Lett. **14**, 196 (1972).
[5] H. van Willigen, M. Plato, R. Biehl, K. P. Dinse, and K. Möbius, Mol. Phys. **26**, 793 (1973).
[6] N. M. Atherton and B. Day, J. Chem. Soc., Farad. II, **69**, 1801 (1973).
[7] H. B. Stegmann, K. Scheffler, G. Bauer, R. Grimm, S. Hieke, and D. Stürner, Phosphorus **4**, 165 (1974).
[8] W. Lubitz, K. P. Dinse, K. Möbius, and R. Biehl, Chem. Phys. **8**, 371 (1975).
[9] R. Biehl, W. Lubitz, K. Möbius, and M. Plato, J. Chem. Phys. **66**, 2074 (1977).
[10] W. Lubitz, R. Biehl, and K. Möbius, J. Magn. Reson. **27**, 411 (1977).
[11] B. Kirste, H. Kurreck, W. Lubitz, and K. Schubert, J. Amer. Chem. Soc., in press.
[12] R. Biehl, Ch. Hass, H. Kurreck, W. Lubitz, and S. Oestreich, Tetrahedron, **34**, 419 (1978).
[13] W. Lubitz, Thesis, Freie Universität Berlin **1977**.
[14] K. P. Dinse, K. Möbius, and R. Biehl, Z. Naturforsch. **28a**, 1069 (1973).
[15] R. Biehl, M. Plato, and K. Möbius, J. Chem. Phys. **63**, 3515 (1975).
[16] D. E. Paul, D. Lipkin, and S. I. Weissman, J. Amer. Chem. Soc. **78**, 116 (1956).
[17] J. Kempf, H. W. Spiess, U. Haeberlen, and H. Zimmermann, Chem. Phys. Lett. **17**, 39 (1972).
[18] W. Schlenk and Margarete Karplus, Chem. Ber. **61**, 1675 (1928).
[19] W. I. Chmelewski and G. I. Fedorow, Chem. Zentralblatt **I**, 862 (1940).

[20] H. E. Ungnade and E. W. Crandall, J. Amer. Chem. Soc. **71**, 3009 (1949).
[21] M. S. Kharasch and H. C. Brown, J. Amer. Chem. Soc. **61**, 2148 (1939).
[22] J. A. Pople and D. L. Beveridge, Approximate Molecular Orbital Theory, McGraw-Hill, New York **1970**.
[23] P. Andersen, Acta Chem. Scand. **19**, 629 (1965).
[24] P. Andersen and B. Klewe, Acta Chem. Scand. **21**, 2599 (1967).
[25] R. Biehl, K. Hinrichs, H Kurreck, W. Lubitz, U. Mennenga, and K. Roth, J. Amer. Chem. Soc. **99**, 4278 (1977).
[26] K. Schreiner, A. Berndt, and F. Baer, Mol. Phys. **26**, 929 (1973).
[27] N. Hirota in Radical Ions, E. T. Kaiser, L. Kevan, Edts., Interscience, New York 1968; K. S. Chen, S. W. Mao, K. Nakamura, and N. Hirota, J. Amer. Chem. Soc. **93**, 6004 (1971).
[28] H. R. Luss and D. L. Smith, Acta Cryst. **B28**, 884 (1972).
[29] W. Lubitz, unpublished results.
[30] D. M. Burns and J. Iball, Proc. Roy. Soc. A **227**, 200 (1955).
[31] J. R. Bolton and G. K. Fraenkel, J. Chem. Phys. **40**, 3307 (1964).
[32] N. M. Atherton, Electron Spin Resonance, Ellis Horwood, Chichester 1973.
[33] J. H. Freed in Electron Spin Relaxation in Liquids, L. T. Muus and P. W. Atkins, Edts., Plenum Press, New York 1972, p. 503.
[34] D. S. Leniart, H. D. Connor, and J. H. Freed, J. Chem. Phys. **63**, 165 (1975).
[35] J. H. Freed, J. Chem. Phys. **43**, 2312 (1965).
[36] H. J. Fey, Diplomarbeit, Freie Universität Berlin 1977.
[37] J. H. Freed, J. Phys. Chem. **71**, 38 (1967).
[38] C. Steelink, L. D. Kispert, J. D. Fitzpatrick, and J. S. Hyde, J. Amer. Chem. Soc. **90**, 4354 (1968).
[39] T. P. Das, J. Chem. Phys. **27**, 763 (1957).
[40] T. Takeshita and N. Hirota, J. Chem. Phys. **51**, 2146 (1969).